UNSUPERVISED CLASSIFICATION OF SEA-ICE USING SYNTHETIC APERTURE RADAR VIA AN ADAPTIVE TEXTURE SPARSIFYING TRANSFORM

Robert Amelard, Alexander Wong, Fan Li, David A. Clausi

Department of Systems Design Engineering, University of Waterloo, Canada

ABSTRACT

A texture sparsifying transform for use in unsupervised classification of sea-ice in polarimetric synthetic aperture radar (SAR) imagery is presented. The goal of the sparsifying transform is to compactly represent the underlying information of the SAR imagery to eliminate sources of unwanted noise and complexities (e.g., banding effect on RADARSAT-2) commonly found in SAR imagery. The proposed algorithm is designed to be simple to implement and discriminative in sea-ice scenes. Performing unsupervised classification on the sparsifying transform space using scenes captured with C-band HV polarization yields experimental results that are much more accurate than common pixel-based methods, and performs comparably to a recent more complex method.

Index Terms— sea-ice classification, sparsifying transform, texture model, synthetic aperture radar.

1. INTRODUCTION

The accurate classification of sea-ice in polar regions is an important task for navigational planning purposes such as ship routing in ice-infested waters. One of the most important tools for monitoring sea-ice conditions in polar regions for navigation planning is spaceborne synthetic aperture radar (SAR) via satellites such as RADARSAT-1 and RADARSAT-2. Operating passively within the microwave spectral range, SAR facilitates the continuous monitoring of sea-ice conditions even under high cloud and snow cover. The classification of sea-ice and water using SAR data has largely been performed manually by trained experts, which is very time-consuming given the large amounts of SAR data being captured daily, as well as subject to human bias. This motivates the development of computer-aided strategies for improving the performance and accuracy of sea-ice and water classification from large volumes of SAR data.

Strategies for sea-ice classification can be grouped into either supervised approaches [1, 2, 3] or unsupervised approaches [4, 5]. Supervised approaches require manually identified training information for learning the underlying classification models. Such approaches require a significant amount of training data and are subject to labeling bias. They also exhibit limited robustness to natural variability in sea-ice and water characteristics being captured in the SAR data, as well as speckle noise. Unsupervised approaches aim to learn the sea-ice and water classes inherent in the raw data irrespective of manual labels. Such approaches hold great promise for operational sea-ice classification as it is more flexible and adaptive to the natural variability in sea-ice and water characteristics, along with variability in the environment and the data acquisition conditions. In this study, we investigated the potential for an adaptive sparsifying transform strategy for unsupervised classification of sea-ice and water using SAR imagery

Thanks to Natural Sciences and Engineering Research Council and the Ministry of Research and Innovation for funding support. RADARSAT is an official mark of the Canadian Space Agency.

2. METHODOLOGY

A novel strategy for unsupervised classification of sea-ice types and/or water using SAR data is proposed based on the concept of an adaptive texture sparsifying transform. First, an adaptive texture sparsifying transform was learned based on a set of texture and spatial representations extracted from the SAR imagery. This transform projects such texture representations into a feature space in which the texture characteristics of the SAR image can be sparsely and compactly represented. Given the learned sparsifying transform, a classifier was then learned (in an unsupervised manner) in this projected sparse feature space to classify between sea-ice types and/or water within the scene. This can be used to predict ice-water coverage in other parts of the scene. The algorithm is presented in pseudocode format in Fig. 3.

3. TEXTURE REPRESENTATIONS

In this work, the local texture characteristics of an $M \times N$ SAR image (denoted as $f(\mathbf{x})$ where $\mathbf{x}$ is the pixel location) is characterized using a set of $M \times N$ neighborhood-based texture representation vectors $\Upsilon = \{\tau(\mathbf{x}_i)\}_i$, for each pixel. Given an r-layer neighborhood centered at pixel $\mathbf{x_i}$, the texture representation vector $\tau(\mathbf{x_i})$ is given by:

$$\tau(\mathbf{x_i}) = \left[f(\mathbf{x_i}) \;\; f(\mathbf{x_i}^{1,1}) \;\; f(\mathbf{x_i}^{2,1}) \;\; \ldots \;\; f(\mathbf{x_i}^{8r,r}) \;\; \mathbf{x_i} \right] \quad (1)$$

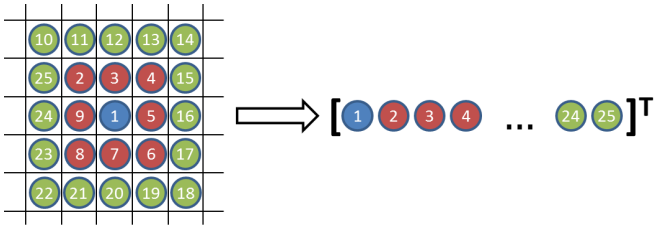

Fig. 1: An example of extracting a texture representation vector from a 2-layer neighborhood using 1, excluding spatial information. The bubbles represent individual pixels in the image, and the numbers represent pixel identiers for illustrative purposes.

where $f(\mathbf{x_i}^{j,k})$ is the pixel intensity at the j^{th} position of the k^{th} layer in the neighborhood centered around pixel location $\mathbf{x_i}$ (see Fig. 1 for an illustrative example). It can be shown that the k^{th} layer in a radial neighborhood has $8k$ pixels in the layer. The last term $\mathbf{x_i}$ in $\tau(\mathbf{x_i})$ provides spatial information to incorporate spatial context into the adaptive texture sparsifying transform learning process. Note that this spatial constraint is only maintained during the sparsifying transform procedure, and is not directly included in the classification stage.

4. ADAPTIVE TEXTURE SPARSIFYING TRANSFORM

We wish to project the set of local texture representation Υ into a feature space in which the texture characteristics of the SAR image $f(\mathbf{x})$ can be sparsely and compactly represented. The sea-ice and water classes may not be well-separated in the original fully-populated feature space, particularly in the presence of natural and imaging variability in sea-ice and water. However, when projected into a feature space where the texture characteristics can be sparsely and compactly represented, the underlying separability between the sea-ice and water classes should improve due to the systematic simplified representation of the data.

Let the feature space in which texture characteristics can be sparsely and compactly represented be defined by a set of vectors forming a basis for this space, which we will denote as $B = \{\mathbf{b_1}, \mathbf{b_2}, \ldots, \mathbf{b_{n_b}}\}$. To learn the set of bases B, we employed a learning strategy based on the minimization of a two-component cost function:

$$B_{\Upsilon,n_b} = \arg\min_{\{\mathbf{b_j}\}} \sum_{j=1}^{n_b} \sum_{\tau(\mathbf{x_i})\in S_j} \Big[\alpha\left(\|\tau^t(\mathbf{x_i}) - \mathbf{b_j^t}\|_2\right) + \beta\left(\|\tau^s(\mathbf{x_i}) - \mathbf{b_j^s}\|_2\right)\Big] \quad (2)$$

where $S_j \subset S$ denotes the set of textural representation vectors being mapped to basis vector $\mathbf{b_j}$, τ^t and τ^s correspond to the texture and spatial components of the representation vector τ, respectively, $\mathbf{b_j^t}$ and $\mathbf{b_j^s}$ corresponds to the texture and spatial components of basis vector $\mathbf{b_j}$, respectively, and α and β control the balance of influence between texture and spatial components.

Given such a feature space, let the texture sparsifying transform $T_B(\tau)$ for SAR image $f(\mathbf{x})$ be defined as a function that maps a texture representation vector $\tau(\mathbf{x_i})$ to one of the basis vectors in B based on a minimum L_2 error norm criterion:

$$T_B(\tau) = \mathbf{b_k}, \text{ s.t. } \left(\|\tau(\mathbf{x_i}) - \mathbf{b_k}\|_2 < \|\tau(\mathbf{x_i}) - \mathbf{b_l}\|_2\right) \quad \forall l \neq k \quad (3)$$

Thus, the adaptive texture sparsifying transform $T_B(\tau)$ can be completely defined by (3) and the learned basis B. The effective result of this sparsifying transform is a pixel map with n_b pixel values such that patches that are spatially and texturally similar are represented by the same pixel value.

5. UNSUPERVISED CLASSIFIER LEARNING

Given the learned adaptive texture sparsifying transform $T_B(\tau)$, the goal is now to learn a classifier in an unsupervised manner within the sparse feature space. At this point, it is wise to only consider the texture components, as classification using the spatial components would misidentify patches that are the same class yet distant from one another. To accomplish this, a minimum L_2 error criterion was used to learn a n_C-class classifier L (corresponding to a set of classifier labels $\mathcal{L} = \{l_1, l_2, \ldots, l_{n_C}\}$ where $\mathcal{L}$ in this case defines ice/water or different types of ice) from $T_B(\tau)$ as follows:

$$L = \arg\min_{C} \sum_{j=1}^{n_C} \sum_{T_B(\tau(\mathbf{x_i}))\in C_j} \|T_B^t\left(\tau(\mathbf{x_i})\right) - \mathbf{\Phi_j}\|_2 \quad (4)$$

where $C_j \subset C$ is the set of basis vectors in B represented by label l_j, $T^t(\tau)$ represents only the texture portion of the basis vector, and $\mathbf{\Phi_j}$ is the prototype for class l_j in the feature space. This can be satisfied using k-means clustering.

6. RESULTS

We used C-band HV polarization SAR imagery acquired by RADARSAT-2 over Chukchi and Beaufort Seas between April and June 2010. These images were chosen since they contain large amounts of noise due to banding effects and the inherent low signal-to-noise ratio of HV imagery, and they incorporate different types of information (Fig. 2a contains two types of ice, and Fig. 2b contains water and ice). For comparison, we generated results using the proposed algorithm, Iterative Region Growing using Semantics (IRGS) [6, 7], k-means, and maximum a posteriori (MAP) using

Gaussian mixture models (GMM) using the same data. The original SAR images were cropped to 600×600 pixels for performance purposes, and we classified into two classes (first-year *vs.* multi-year ice for Fig. 2a, and ice *vs.* water for Fig. 2b). For testing purposes we used 2-layer neighborhoods (i.e., 5×5 pixel neighborhoods), $\alpha = 1$, $\beta = 10$, and $n_b = 1000$ bases. For computational reasons, the adaptive texture sparsifying transform was performed on the scene in distinct partitions. That is, we analysed the scene in 30×30 pixel partitions prior to the classification stage.

Visual results are presented in Fig. 2. Fig. 2a comprises two types of ice: first-year (dark) and multi-year (light) ice. The proposed method properly grouped the types of ice into cohesive structures, as opposed to pixel-based methods which produced very localized classifications of the types of ice. This is especially observed in the bottom part of the image, where small pixel clusters were erroneously determined to be multi-year ice. The proposed method generated very similar classification maps to IRGS (Fig. 2c–2d).

Fig. 2b comprises ice and water in the scene. The proposed method again generated pixel labels that are coherent, as opposed to the k-means and MAP methods that produced scattered pixel labels both in the water and on the ice. The banding effects, which are especially viewable in the bottom-right of the image, were properly interpreted by the proposed method, whereas the pixel-based methods identified the peaks of the bands as ice. This hints at the discriminative power of analysing patches rather than per-pixel analysis.

In both of these scenes, the proposed method has shown improvements over pixel-based methods, and is comparable to the recent IRGS method. However, the implementation of the proposed method is simpler than that of IRGS. IRGS requires initializing and updating a region adjacency graph across the entire scene, and uses simulated annealing as the iterative optimization technique. The proposed method relies only on a sliding window approach and k-means clustering, both of which are common image processing techniques.

7. CONCLUSIONS

In this paper we have proposed an adaptive texture sparsifying transform for performing unsupervised classification to differentiate sea-ice/water and ice types using a single HV polarization SAR image. This transform projects the SAR pixel data into a sparse feature space where the underlying classes are much more separable and well-defined. Classification using this sparse feature space is more likely to converge to a desirable solution as the data is systematically simplified using commonly observed textural representations. The experimental results indicate that the proposed method performs better than benchmark pixel-based methods, and performs comparably to a recent more complex method on the same data.

I – Image
r – Patch Size
α, β – Spatial/Texture Weights
$n_C/n_B/n_P$ – Number of Classes/Texture Bases/Partitions

function SEAICECLASSIFICATION(I, r, α, β, n_C, n_B, n_P)
  $M \leftarrow \emptyset$
  for each partition **do**
    $\Upsilon \leftarrow \{\tau(\mathbf{x_i})\}\ \forall$ pixels $\mathbf{x_i}$
    Learn $B_{\Upsilon, n_B/n_P}$
    for each pixel $\mathbf{x_i}$ **do**
      $M(\mathbf{x_i}) \leftarrow T_B(\tau(\mathbf{x_i}))$
    end for
  end for
  Learn L using M
end function

Fig. 3: Proposed Algorithm

8. REFERENCES

[1] A. Bogdanov, "Neuroinspired architecture for robust classifier fusion of multisensor imagery," *IEEE Trans. Geosci. Remote Sens.*, vol. 46, no. 5, pp. 1467–1487, 2008.

[2] Q. Yu and D. A. Clausi, "SAR sea-ice image analysis based on iterative region growing using semantics," *IEEE Trans. Geosci. Remote Sens.*, vol. 45, no. 12, pp. 3919–3931, 2007.

[3] L.-K. Soh, C. Tsatsoulis, S. Member, D. Gineris, and C. Bertoia, "ARKTOS: An intelligent system for SAR sea ice image classification," *IEEE Trans. Geosci. Remote Sens.*, vol. 42, no. 1, pp. 229–248, 2004.

[4] R. Kwok, E. Rignot, and B. Holt, "Identification of sea ice types in spaceborne synthetic aperture radar data," *J. Geophysical Research*, vol. 97, no. C2, pp. 2391–2402, 1992.

[5] S. Ochilov and D.A. Clausi, "Operational SAR sea-ice image classification," *IEEE Trans. Geosci. Remote Sens.*, vol. 50, no. 11, pp. 4397–4408, 2012.

[6] Q. Yu and David A. Clausi, "SAR sea-ice image analysis based on iterative region growing using semantics," *IEEE Trans. Geosci. Remote Sens.*, vol. 45, no. 12, pp. 3919–3931, 2007.

[7] Q. Yu and David A. Clausi, "IRGS: Image segmentation using edge penalties and region growing," *IEEE Trans. Pattern Anal. Mach. Intell.*, vol. 30, no. 12, pp. 2126–2139, 2008.

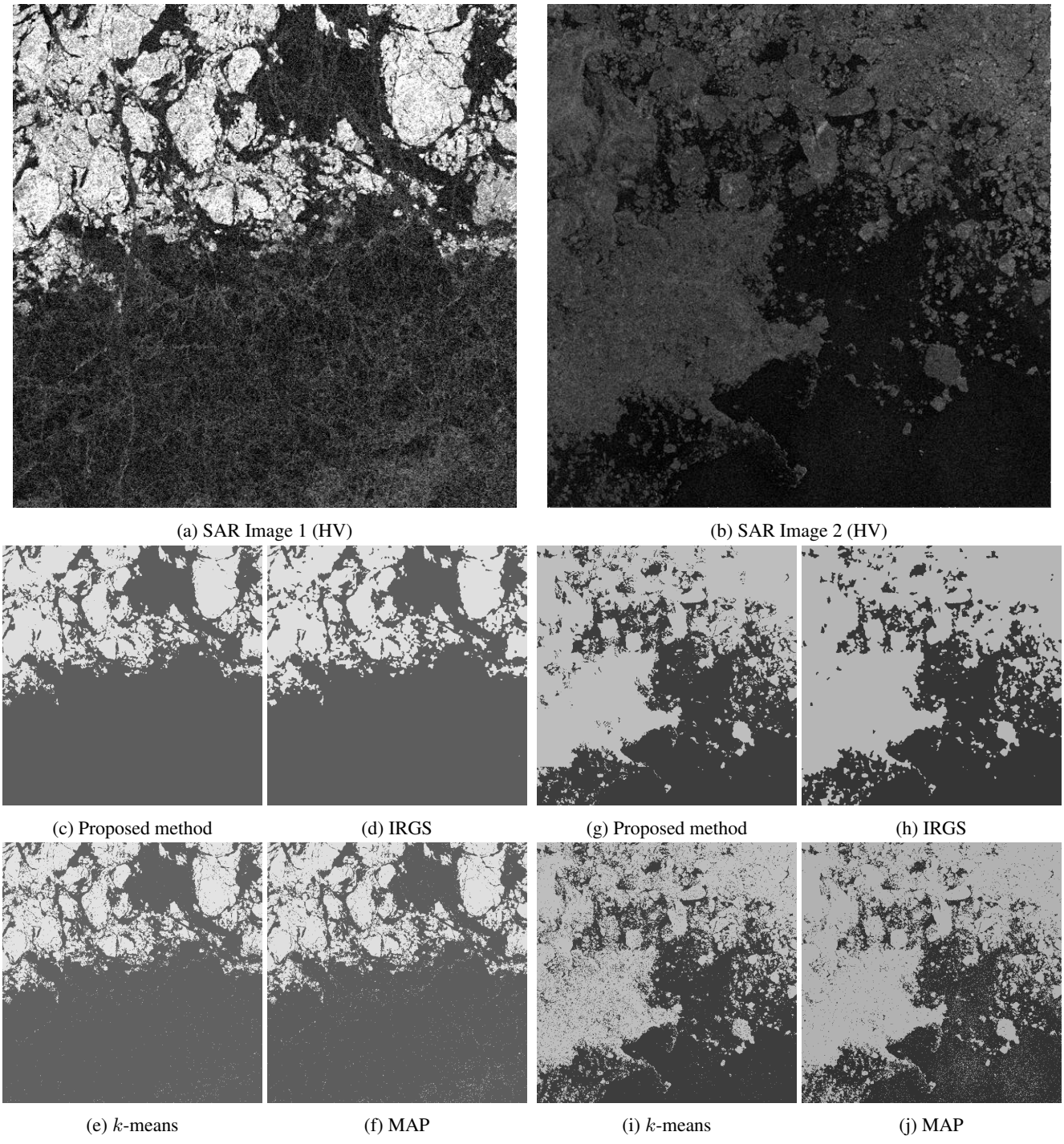

(a) SAR Image 1 (HV)

(b) SAR Image 2 (HV)

(c) Proposed method

(d) IRGS

(g) Proposed method

(h) IRGS

(e) k-means

(f) MAP

(i) k-means

(j) MAP

Fig. 2: Sample sea-ice classification results using RADARSAT-2 C-band HV SAR imagery. The proposed method is not privy to banding effects or small localized misclassifications like k-means and MAP, and it also performs comparably to the more complex IGRS method.

(a) Apr 18 2010, 21–28° incidence angle.

(b) Jun 29 2010, 22–29° incidence angle.